We are IntechOpen, the world's leading publisher of Open Access books Built by scientists, for scientists

6,900
Open access books available

186,000
International authors and editors

200M
Downloads

Our authors are among the

154
Countries delivered to

TOP 1%
most cited scientists

12.2%
Contributors from top 500 universities

WEB OF SCIENCE™

Selection of our books indexed in the Book Citation Index in Web of Science™ Core Collection (BKCI)

Interested in publishing with us?
Contact book.department@intechopen.com

Numbers displayed above are based on latest data collected.
For more information visit www.intechopen.com

Chapter

Organic Thermoelectrics and Thermoelectric Generators (TEGs)

Lazaros Tzounis

Abstract

Inorganic and organic thermoelectric (TE) materials have received an extensive scientific interest during the last decades, due to their ability to directly convert the thermal energy to electricity. This is described by the well-known "Seebeck effect". TE materials can convert also electricity into cooling through the "Peltier effect". As such, TE materials and thermoelectric generator (TEG) devices can be utilized for potential applications including (i) thermal energy harvesting, (ii) local cooling and (iii) temperature sensing. The direct conversion of heat into electricity has been one of the most attractive solutions to the severe environmental and energy issues the humanity is coming across. This chapter covers the fundamental working principle of TE materials, the synthetic protocols for inorganic and organic thermoelectric materials, techniques and technologies for the fabrication of thermoelectric generators (otherwise defined as thermoelectric module devices) and a number of applications. Finally, future aspects and outlooks for further advancements at the "material" or "device" level for efficient power generation are remarked.

Keywords: Seebeck coefficient, thermoelectric (TE) nanomaterials, organic thermoelectrics, thermoelectric generators (TEGs)

1. Introduction to energy needs and wasted thermal energy

Due to the finite supply of fossil fuels and the human-induced global climate change, an emerging energy crisis has been realized in the twenty-first century giving rise to the exploitation of "green" energy and alternative energy resources [1–3]. There has been a substantial increase in the consumption of energy resources and especially that of petroleum feedstocks mainly due to (i) the industrial development and (ii) population growth [4]. In industrial environments and our daily life, large amounts of the generated heat energy cannot be effectively used getting inevitably wasted in the environment, e.g. emissions of factory boilers, car exhausts, friction, etc. A major contributor to waste heat is the transport sector, where only the 20% of the fuel's energy ends up as useful energy. Relatively, aeronautics and automotive are examples of high energy usage with low efficiency, where roughly 75% of the energy produced during combustion is lost in the turbine/exhaust or engine coolant in the form of heat. In relation, more than 60% of the energy produced in the USA is never utilized, as most of it is dissipated in the form

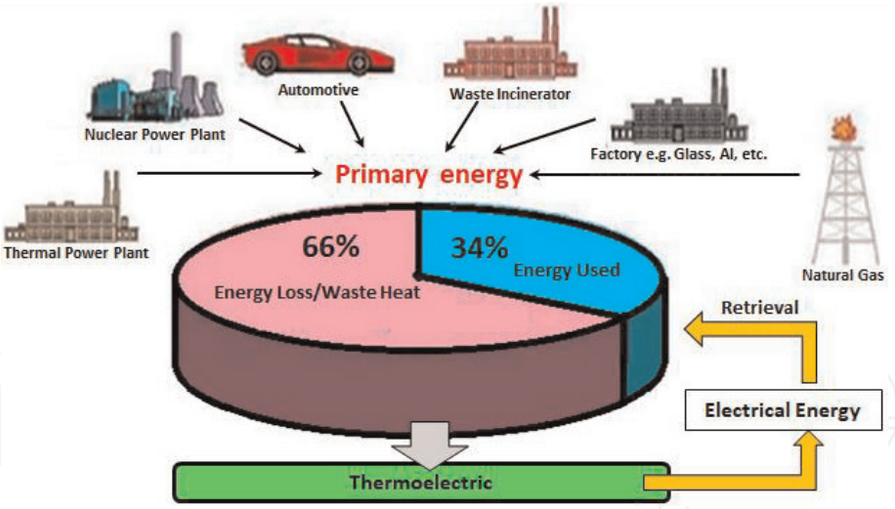

Figure 1.
Schematic representation of different sectors contributing to large amounts of wasted thermal energy.

of waste heat [5]. **Figure 1** shows the average effectively used energy from fossil fuels, while it represents schematically the different sectors that large amounts of waste heat are generated and could be transformed to electrical energy via the deployment of thermoelectric (TE) materials. Thus, a key solution for the huge amounts of wasted thermal energy (>60%) will be energy-harvesting technologies to effectively recycle and partially or fully harvest this inevitably generated and regrettably wasted thermal energy. Besides searching for alternative energy sources, for instance, solar energy, thermal energy, wind energy, hydrogen energy and biomass energy, to replace the conventional fossil fuels, improving the current efficiency of energy use is undoubtedly an expedient and viable solution.

2. Fundamentals of the thermoelectric effect and thermoelectric materials

The thermoelectric effect, otherwise known as "Seebeck effect", is the direct conversion of a temperature difference between two dissimilar electrical conductors or semiconductors to an electrical voltage. When the sides of TE materials are exposed to different temperatures, then a voltage is created across the two sides of the material. Conversely, when a voltage is applied, a temperature difference can be created, known as the "Peltier effect". At the atomic scale, when a temperature gradient is applied at the two end sides of a thermocouple, the electrons and holes move faster, and they have a lower density at the hot side, resulting in diffusion of electrons/holes towards the cold side as schematically demonstrated in **Figure 2**. This movement of carriers (electrons for n-type and holes for p-type materials) is translated into the generation of an electric field across the thermocouple. This is called as the "Seebeck effect", and the voltage created for a temperature difference, ΔT, under thermodynamic equilibrium is $S \times \Delta T$, where S is the Seebeck coefficient. TE materials are therefore one potential candidate for harvesting waste thermal energy, due to their ability to convert it into electricity, even under very-low-temperature gradients relative to the environmental temperature. This technology exhibits distinct advantages over other energy-harvesting technologies: (i) TE conversion is reliable and operates in silence as it works without mechanical movement, (ii) it is an environmentally friendly green technology, since no heat and no gaseous or chemical wastes are produced during operation, and (iii) it can be widely

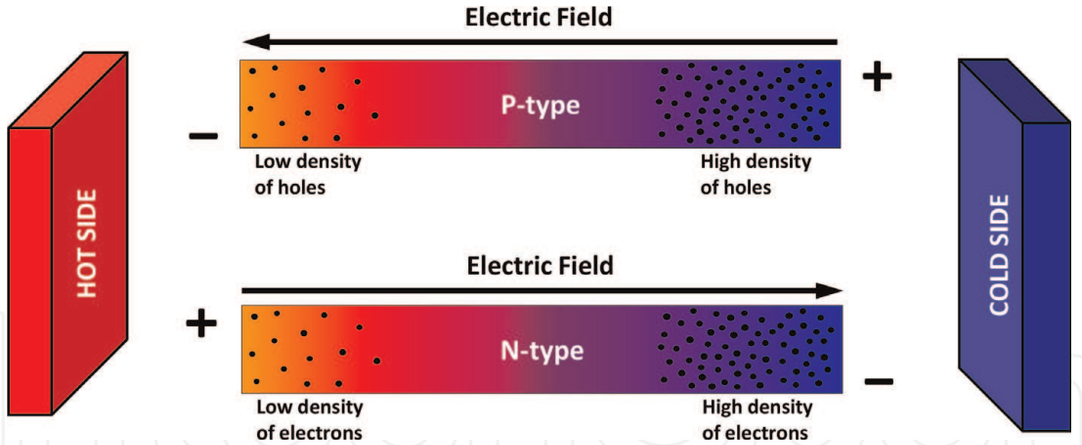

Figure 2.
A schematic representation of the TE effect showing the charge carriers of a p- or an n-type material to diffuse from the hot side to the cold, when a temperature gradient is applied.

used in places where other energy conversion technologies are unavailable, such as in the remote outer space, etc. [6, 7].

The "thermoelectric effect" encompasses three distinct effects: (a) the Seebeck effect, (b) the Peltier effect and (c) the Thomson effect. The Seebeck and Peltier effects are different manifestations of the same physical process, while it is often referred to as the Peltier-Seebeck effect. The Thomson effect is an extension of the Peltier-Seebeck model and is credited to Lord Kelvin. Seebeck in 1821 created a circuit made from two dissimilar metals; copper (Cu) and bismuth (Bi), while upon exposure the two end-junctions at different temperatures (hot/cold), he observed that the applied temperature gradient generated a voltage (experimentally observed that a compass magnet was deflected), which is commonly referred to then as the Seebeck effect [8]. Later, in 1834 Peltier observed that when an electric current flows through Cu and Bi wires at room temperature, a temperature difference could be created, and this is known onwards as the Peltier effect widely deployed in the refrigeration processes [9]. The Seebeck effect provides a theoretical basis for the applications of thermoelectric energy converters (energy harvesting), while the Peltier effect for cooling devices (refrigeration). To date, TE materials have been widely used in several high-tech applications such as aerospace, military, medical thermostats, microsensors, wearables, etc.

TE materials obey the thermoelectric or Seebeck effect described by the thermoelectric power (TEP), or thermopower, or Seebeck coefficient (S) [10]. The Seebeck coefficient is defined then as shown in Eq. (1):

$$S = \frac{\Delta V}{\Delta T} \tag{1}$$

where ΔV is the electric potential difference or the generated thermovoltage created by a temperature gradient, ΔT. It is an intrinsic material property related to the electronic properties, and it is positive for p-type and negative for n-type semiconductors [11]. The Seebeck coefficient is used for the calculation of the power factor ($PF = \sigma \times S^2$) (σ is the electrical conductivity), a well-known entity for comparing the voltage output (V_{out}) of different TE materials. The efficiency of TE materials is characterized by a dimensionless figure of merit (ZT); $ZT = (\sigma \times S^2/\kappa) \times T$, where σ represents the electric conductivity (S/m), S the Seebeck coefficient (μV/K), κ the material's thermal conductivity (W/mK) and T the absolute temperature (K) [12].

In recent years, great progress has been made in improving the ZT. It could be realized that an efficient TE material should exhibit high electrical conductivity

combined with high Seebeck coefficient and low thermal conductivity. The Seebeck coefficient S, characteristic of the average entropy per charge transport, should be large in order to create a high voltage induced by a temperature gradient. The Seebeck coefficient, however, is not the only parameter to be optimized in order to maximize ZT. The electrical conductivity (σ) must be large to minimize the Joule heating during charge transport. Apart from the two parameters mentioned, a good TE material should exhibit also low thermal conductivity (κ), to prevent heat flow through the material. These three factors are interdependent in bulk TE materials, and altering one changes the other two. The difficulty in simultaneously optimizing them causes TE research to decay, until great reduction of thermal conductivity were both theoretically and experimentally proven in nanomaterials in 1993 [13]. The difficulty of designing high-performance TE materials arises from the fact that both electrical and thermal conductivities are related via the carrier concentration and, thus, optimizing one parameter will negatively affect the other. This interdependence has delayed the development of TE materials for many years.

Although TE technology possesses many merits and has been known for two centuries, it has only been applied in narrow fields because of its low conversion efficiency (typically less than 6%) [14]. The conversion efficiency strongly depends on the ZT of TE materials, as described by Eq. (2):

$$n = n_c \frac{\sqrt{1+ZT}-1}{\sqrt{1+ZT}+\frac{T_c}{T_h}} \tag{2}$$

where n is the conversion efficiency of heat to electricity; T_c and T_h are the temperatures of cold and hot sides of a TE material, respectively; and n_c represents the Carnot efficiency expressed as $n_c = 1 - T_c/T_h$ or $(T_h - T_c)/T_h \times 100\%$. It can be clearly realized that ZT should be at least above 3 in order to ensure that the TE material/device conversion efficiency is competitive with that of traditional power generators, which can reach 40% of Carnot efficiency [15]. The electrical conductivity (σ) being an important factor in the ZT equation can be expressed by Eq. (3):

$$\sigma = n\, e\, \mu \tag{3}$$

where n is the charge carrier density or concentration, μ is the mobility of charge carriers and e is the charge of unit carrier (electron or hole).

The electrical conductivity can be improved via chemical doping that each dopant atom can have one more valence electron than its host atoms and can therefore facilitate the increase of charge carrier density. Meanwhile, the dopants can reduce the mobility of charge carriers due to the enhanced scattering between dopants and carriers. The ideal density of charge carriers has been reported to be in the range of 10^{19} to 10^{21} cm^{-3} [16].

Doping improves also the Seebeck coefficient by changing the electron density of states (DOS) [17]. As shown in Eq. (4), the Seebeck coefficient is mainly affected by the charge carrier concentration, as well as the effective mass of the charge carriers (m^*), which usually decreases with increasing carrier mobility (k_B and h are the Boltzmann constant and Planck constant, respectively):

$$S = \frac{8\,\pi^2 k_B^2}{3\,e\;h^2} m^* T \left(\frac{\pi}{3n}\right)^{\frac{2}{3}} \tag{4}$$

The thermal conductivity is decreased by phonon scattering (e.g. phonon-boundary scattering, phonon-defect scattering and phonon-phonon scattering).

The thermal conductivity is the summation of two components: (i) the electron thermal conductivity (k_e) and (ii) the lattice thermal conductivity (k_c), as can be expressed in Eq. (5):

$$k = k_e + k_c \tag{5}$$

k_e is proportional to the electrical conductivity according to the Wiedemann-Franz law [18]. In semiconductors, usually >90% of thermal conductivity arises from the lattice thermal conductivity (k_c), which is independent of the electrical conductivity. Hence, reducing the lattice thermal conductivity will lead to a pronounced enhancement of the TE performance.

Then, the dimensionless "figure of merit", ZT, could be rewritten as shown in Eq. (6):

$$ZT = \left\{ \left[\frac{8\,\pi^2 k_B^2}{3\,q\;\;h^2} m^* T \left(\frac{\pi}{3n} \right)^{\frac{2}{3}} \right]^2 \right\} \left(\frac{\mu}{k} \right) qT \tag{6}$$

where S, σ, k and T are the Seebeck coefficient, electrical conductivity, thermal conductivity and absolute temperature, respectively; k_B is the Boltzmann constant; h is Planck's constant; q is the charge; n is the charge carrier concentration; μ is the mobility and m^* is the effective mass of the charge carrier.

From the above, it could be realized that the Seebeck coefficient, thermal conductivity and electrical conductivity are strongly dependent, and it is therefore very challenging to improve them simultaneously in bulk TE materials. This is mainly the reason that very few researches exist on TE materials from the 1960s to the 1990s, until the article was published in 1993 by Dresselhaus and co-workers showing theoretically that low-dimensional materials can have higher ZT than their bulk analogues, due to both their lower thermal conductivity and quantum confinement effects [19, 20]. This work triggered the scientific community research interest in TE materials and provided a mainstream approach and strategy for the enhancement of TE material's performance and ZT values. This can be achieved more precisely via creating proper material "nanostructuring" inducing a large number of interfaces and facilitating thus a phonon scattering resulting into low thermal conductivity values. The TE material's research and the promising nanostructuration approaches are part of the wider field of nanotechnology, where key elements are the long-range ordering with controlled nanostructures for enhanced optical [21–29], electrical [30–39], mechanical [40–42] and magnetic [43, 44] properties.

Figure 3 demonstrates the number of publications on TE materials from 1965 to today, highlighting the slight increase of TE research rate from 1965 to 1993 and the rapid increase from that year to now, due to the flagship stimulating work of Dresselhaus (data collected from Science Direct data library using "thermoelectric" as the keyword). The extreme interest for TE materials during the last decades, mainly during the last decade, has been the driving force for many review articles that have appeared focusing on the different types of TE materials [45–51] including oxide [45] and organic based [47]. For example, Sootsman et al. summarized new and old concepts in inorganic TE materials in 2009 [48]. M. S. Dresselhaus and co-workers had reviewed in 2007 new directions for low-dimensional inorganic TE materials [13]. Li et al. highlighted progress in TE materials with high ZT and the related fabrication processes for producing nanostructured materials including Bi-Te alloys, skutterudite compounds, Ag-Pb-Sb-Te quaternary systems, half-Heusler compounds and high ZT oxides [52]. The last decade, reviews on organic-based TE materials and devices have appeared. Relatively, Du et al. reviewed in

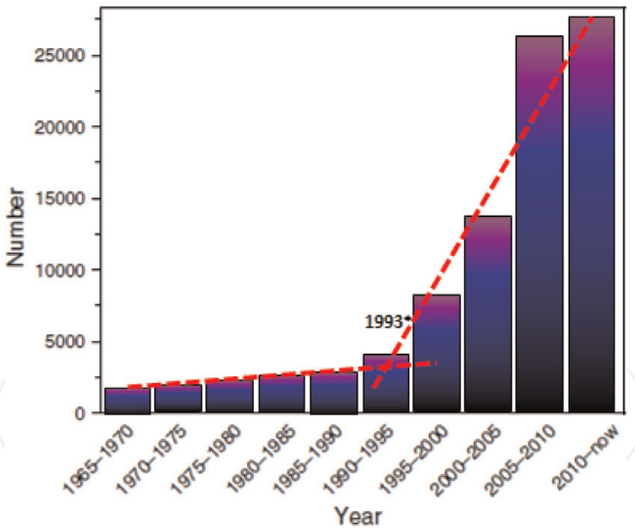

Figure 3.
The number of publications in the area of thermoelectric materials and related technology from 1965 to today. The data were collected from science direct data library using "thermoelectric" as the keyword.

2012 the research progress on polymer-inorganic TE nanocomposite materials [53]. Gao et al. summarized in 2016 the conducting polymer/carbon particle TE nanocomposites as emerging green energy materials [54]. Chen et al. reviewed in 2017 advances in polymer TE composites [55]. A very important review by He et al. in 2017 had summarized all the state-of-the-art TE devices, architectures, geometries, device interconnections, contact optimization, etc., based on inorganic and organic (small molecule, polymer, micro- and nanocomposites) TE materials [56]. Finally, it is worth mentioning that, currently, the highest value of ZT (ZT = 3.6 at 580 K) has been reported by Harman et al. for $PbSe_{0.98}Te_{0.02}$/PbTe quantum dot superlattices (QDSLs) grown by molecular beam epitaxy (MBE) [57].

3. Organic thermoelectrics: polymer and nanocomposite systems

3.1 Conjugated polymer thermoelectric materials

Organic thermoelectric (OTE) materials or "organic thermoelectrics" have attracted an increased scientific interest as an alternative approach to conventional inorganic thermoelectrics. Conducting polymers have been suggested as TE materials for potential large-area thermoelectric applications. This is because OTEs are compatible with inexpensive, large-scale processing methods and often possess unique mechanical flexibility, which makes them geometrically versatile to be integrated in complex three-dimensional (3D)-shaped objects, e.g. wearables, car roofs, etc.

Till now, polyaniline (PANI) has been the most studied conductive polymer due to its high electrical conductivity, good chemical and thermal stability and ease of preparation and processing/casting from solution. Poly(3,4-ethylenedioxythiophene):polystyrenesulfonate (PEDOT:PSS) is the second most used polymer with potential processability from water dispersions that are commercially available, good charge transport properties (both of electronic carriers, as well as ions) resulting in relatively high electrical conductivities. However, PEDOT:PSS exhibits low resistance to humid environments due to its hygroscopic behaviour arising from the PSS phase.

In 2002, the first study appeared in literature reporting on the use of electrically conductive polymers and especially polyaniline films as organic thermoelectric

(OTE) materials [58]. OTEs are particularly attractive for low-quality waste heat harvesting such as waste heat at low temperatures. Till then, high *ZT* values (>0.1) have been achieved for both p-type and n-type OTE materials [59, 60]. Similarly to inorganic thermoelectrics, organic ones should be also optimally "electronic crystals and phonon glasses". The main crucial parameter to tune and optimize for organic thermoelectrics is to achieve "electronic crystals", since their thermal conductivities are intrinsically relatively low. Therefore, the thermoelectric parameter to put effort on and optimize is the power factor, via simultaneously increasing the electrical conductivity and Seebeck coefficient. The Seebeck coefficient is directly related to the DOS as stated several times in this chapter, reflecting the average entropy transported per charge carrier. As such, it decreases with increasing carrier concentration since the mobility is decreased. On the contrary, the electrical conductivity increases with carrier concentration, n, and carrier mobility μ ($\sigma = ne\mu$).

Organic semiconductors have been largely neglected as TE materials, despite their inherent low thermal conductivities (≈0.3 W/mK) and high electrical conductivities (>1000 S/cm) [47]. This is due to the fact that conducting polymers are not stable at high temperatures with their maximum operational temperatures limited in the range of 200–250°C. Hence, the benchmark for polymer-based thermoelectrics is Bi_2Te_3 alloys that exhibit a *ZT* of 1.2 at room temperature [61].

Conjugated polymers and mainly PANI [62–64] and polythiophenes [65–69] have been investigated as OTE materials. **Figure 4** depicts the molecular structures of representative p- and n-type semiconducting polymers and dopants, associated with the power factor values that have been experimentally determined.

The most used p-type polymeric material investigated till now is the blend of poly(3,4-ethylenedioxythiophene):polystyrenesulfonate which has been utilized in various organic electronic devices, e.g. OPVs, OTFTs, OTEs, OLEDs, etc. PEDOT:PSS is a polyelectrolyte consisting of positively charged PEDOT and negatively charged PSS. Crispin et al. reported power factors of 300 μW m^{-1} K^{-2} and *ZT* values of 0.25, after de-doping highly conductive PEDOT:tosylate with tetrakis (dimethylamino)ethylene [47]. Besides, the addition of carbon nanotubes (CNTs) or graphene is a popular approach to modulate the TE properties of PEDOT:PSS

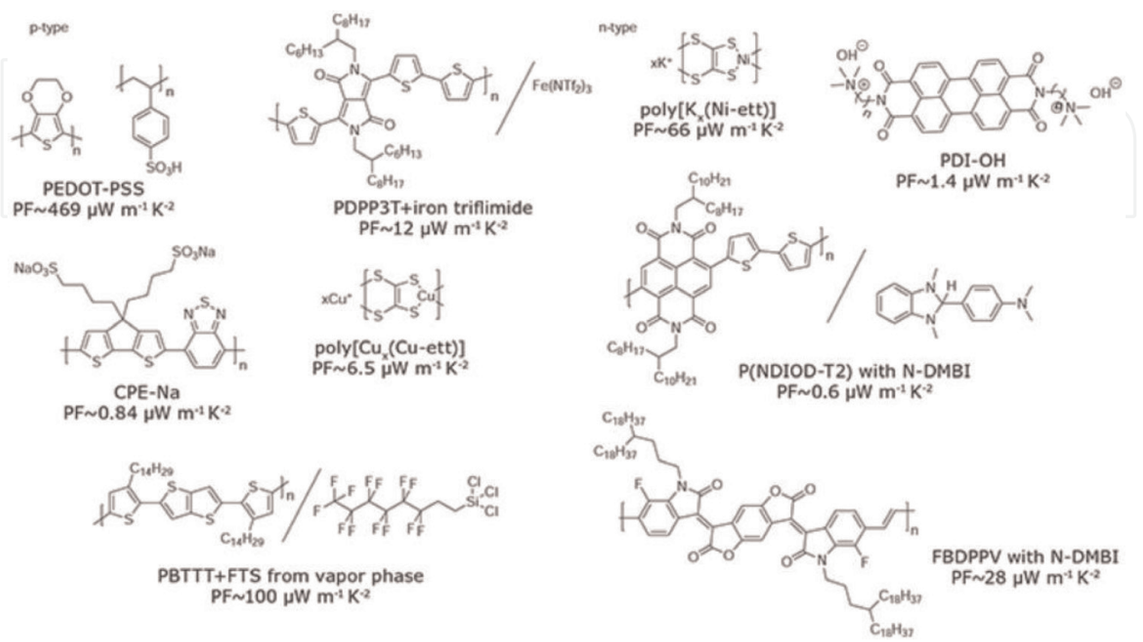

Figure 4.
Representative p-type and n-type semiconducting polymers and dopant materials together with the respective power factors.

[70]. By carefully structuring the composite film, conductivities of 105 S/m and Seebeck coefficients of 120 μV/K were measured, leading to power factors of 2710 μW m^{-1} K^{-2}, one of the highest values reported for OTE materials.

While the p-doping of organic semiconductors can be readily achieved, n-doping is more challenging. Organic electron-deficient semiconductors are associated with the high electron affinities (−3 to −4 eV), making the negatively charged molecules prone to reactions with environmental moisture or oxygen [71]. The charge transfer co-crystal salt of tetrathiafulvalene (TTF) and tetracyanoquinodimethane (TCNQ) is probably the most studied charge transfer salt showing promising n-type thermoelectric properties. Electrical conductivities of 500 S/cm and power factors of up to 40 μW m^{-1} K^{-2} have been reported. However, several drawbacks significantly limit the applicability of charge transfer crystals as TE materials, e.g. modulating the carrier densities is difficult since the stoichiometry of the co-crystals must be accurately respected and the physical properties of the co-crystals are not isotropic. Alternative n-type conductors for TE applications have mainly focused on the perylenediimide- and naphtalenediimide-containing organic semiconductors. Segalman et al. synthesized a series of perylenediimide (PDI)-based molecular semiconductors functionalized with tertiary amine-containing side chains [72]. Upon thermal annealing, the functionalized PDI moieties self-dope via a dehydration reaction of the tethered tertiary ammonium hydroxide. By carefully designing the side chains, the self-doped PDI moieties achieve conductivities of 0.5 S/cm and power factors of 1.4 μW m^{-1} K^{-2}. Chabinyc et al. extrinsically doped the high-performing n-type polymer poly(N,N′-bis(2-octyldodecyl)-1,4,5,8-napthalenedicarboximide-2,6-diyl]-alt-5,5′-(2,2′-bithiophene)) (P(NDIOD-T2) with the molecular dopant (4-(1,3-dimethyl-2,3-dihydro-1H-benzoimidazol-2-yl) phenyl) (N-DMBI) [73]. While the conductivity initially increases as a function of dopant loading, a sharp drop in conductivity was observed at higher loadings. The miscibility of the N-DMBI dopant in the polymer phase is limited, which is why at higher dopant loadings, the dopant crystallizes and phase separates from the polymer matrix, thus reducing the doping efficiency. Despite the morphological instabilities, Seebeck coefficients of −850 μV/K have been achieved with power factors of 0.6 μW m^{-1} K^{-2}. In a recent report, Pei et al. showed that BDOPV-based FBDPPV polymers have reached a record power factor of 28 μW m^{-1} K^{-2} [74]. Huang et al. reported that thiophene-diketopyrrolopyrrole-based quinoidal (TDPPQ) can exhibit a high power factor of 113 μW m^{-1} K^{-2}, when the material is interfacially doped by the bismuth. The performance is the best value for all reported n-type small molecules [75].

3.2 Nanocomposite polymer thermoelectric materials

Nanocomposite polymer thermoelectrics using a conducting and nonconducting matrix and organic (e.g. CNTs, graphene oxide, fullerenes, etc.) or inorganic nanoinclusions (e.g. Bi_2Te_3, PbTe, Te nanowires, etc.) have been also extensively studied.

PEDOT:PSS (CLEVIOS PH1000) mixed with Bi_2Te_3 particles have reached power factors ($PF = \sigma \times S^2$, where σ is the electric conductivity and S the Seebeck coefficient) in the range of ∼130 μW/m K^2 [76]. The incorporation of CNTs may enhance their performance via increased conductivity or molecular orientation effects of the polymer chains. Thereby, high filler loadings (>> 50 wt.%) can be realized [77], resulting in high electrical conductivities [78–81]. Namely, electrical conductivities up to 4×10^5 S/m and power factors in the range of ∼140 μW m^{-1} K^{-2} have been reported by Moriarty et al. for single-walled carbon

nanotubes (SWCNTs) in a PEDOT:PSS matrix [68]. However, the low thermal and moisture stability of these materials is an impediment to engineering and structural applications.

CNTs have been introduced also via solution and melt-mixing methods in engineering nonconductive thermoplastic polymer matrices resulting into nanocomposites with thermal energy-harvesting property [82–86]. Polymer nanocomposites are attractive organic materials due to their ease of production, relatively low cost, flexibility and high specific properties [30–33, 87, 88]. SWCNT polycarbonates (PC)/SWCNT nanocomposites prepared by solvent mixing showed that by increasing the SWCNT content (up to 30 wt.%), the electrical conductivity increases to approximately 1000 S/m, and the Seebeck coefficient reaches 60 μV/K with only a slight dependence on the SWCNT content. CNT composites with polymers having electron-rich functional groups, like PVA and polyethyleneimine (PEI), have been found to act as n-doping to the incorporated SWCNTs and resulted in coefficients up to −21.5 μV/K. Antar et al. reported on melt-mixed composites of polylactide (PLA) with multi-walled carbon nanotubes (MWCNTs) and expanded graphite with high filling levels (up to 30 wt.%) resulting in electrical conductivities of ~4000 S/m [89]. The Seebeck coefficient reached a maximum of 17 μV/K for the composites with expanded graphite and ~9 μV/K for MWCNT ones. Research from our group using a series of melt-mixed polycarbonate-MWCNT nanocomposites has shown that an increasing filler content results in an increase of the power factor due to the increase of the electrical conductivity [36, 90, 91]. The TE properties of melt-mixed conductive nanocomposites of polypropylene (PP) filled with single-walled carbon nanotubes (2 wt.%) and copper oxide (5 wt.%) showed that by adding polyethylene glycol (PEG) during melt mixing p-type composites switched into n-type with Seebeck coefficient up to +45 μV/K and −56 μV/K, respectively [86].

Hierarchical CNT-coated fibrous reinforcement structures have been reported also as TE reinforcements upon their incorporation in polymer matrices for potential large-scale thermal energy harvesting by structural composites, e.g. in aerospace and automotive [34, 42]. Most of the polymeric matrices studied so far are based on aliphatic or semi-aromatic backbones. This severely limits their applicability as engineering materials capable of operating in high-temperature environments.

High-performance engineering polymers such as all-aromatic polyimides and poly(ether-imide)s (PEIs) are capable of withstanding high temperatures (>200°C) and exhibit glass-transition temperatures (T_g) above 200°C with superlative mechanical properties. Recently, Tzounis et al. [38] demonstrated the first synthesis of all-aromatic PEI-SWCNT nanocomposite films as thermoelectrics.

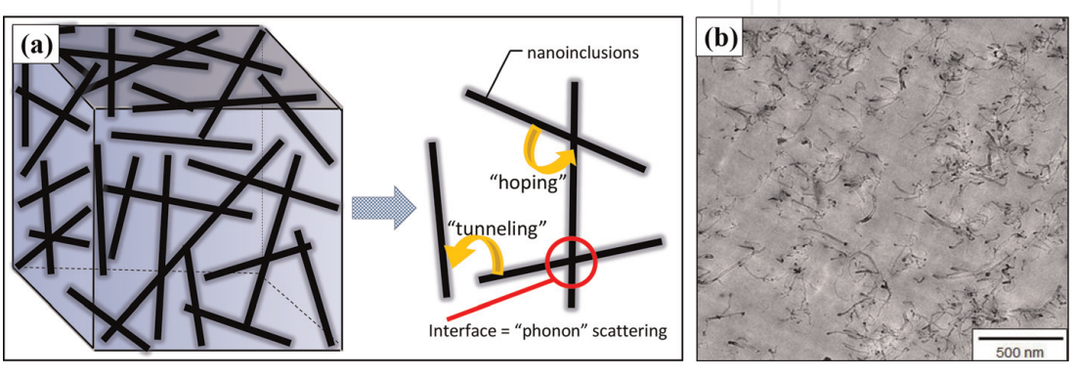

Figure 5.
(a) Schematic representation of the mechanism based on electronic charge transport that governs the TE effect upon exposure to a temperature gradient and (b) a TEM image of a polymer/CNT nanocomposite.

Polymer	Nanofiller	Preparation method	σ (S/cm)	S (μV/K)	PF (μW m^{-1} K^{-2})	κ (W m^{-1} K^{-1})	ZT (T)	Ref.
Polyacetylene	—	Casting	4.990–11.560	11.4–28.4	—	0.7	0.0047–0.38 (300 K)	[101]
Polypyrrole	—	Casting	100	12	—	0.1–0.2	0.002 (300 K)	[101]
Polypyrrole	rGO (67 wt.%)	In situ chemical polymerization	41.6	26.9	3.01 (300 K)	—	—	[102]
Polyaniline (PANI)	—	Casting	7.000	7	—	0.1–0.2	0.051 (300 K)	[101]
Polyaniline (PANI)	GNs (30 wt.%), HCl	In situ chemical polymerization	38	26	2.6 (453 K)	0.6	1.95×10^{-3} (453 K)	[103]
Polyaniline (PANI)	Bi_2Te_3	Solution mixing	60	110	5.1 (350 K)	—	0.18 (350 K) estimated	[104]
Polythiophene	—	Casting	100	21	—	0.1–0.2	0.0066 (300 K)	[101]
Poly(para-phenylene)	—	Casting	10^{-5}	12	—	0.1–0.2	2.1×10^{-10} (300 K)	[101]
Poly(p-phenylene vinylene)	—	Casting	10^{-5}	7	—	0,1–0,2	$7{,}2 \times 10^{-11}$ (300 K)	[101]
Poly(carbazolenevinylene)	—	Casting	5×10^{-3}	230	—	0.1–0.2	8×10^{-5} (300 K)	[101]
PEDOT:PSS	—	Casting	55	13	—	0.1–0.2	0.0014 (300 K)	[101]
PEDOT:PSS	—	Casting	900	75	—	0.24	0.42 (300 K)	[101]
PEDOT:PSS	rGO (21 wt.%)	Mixing	715.03	22.9	32.4 (300 K)	~0.2	0.067 (300 K)	[105]
PEDOT:PSS	Graphene (2 wt.%)	Solution spin casting	32.13	58.77	11.09 (300 K)	0.14	0.021 (300 K)	[106]
PEDOT:PSS	Fullerene (9%) rGO (16%)	In situ chemical polymerization	50.8 ± 5.9	31.8 ± 2.3	5.2 ± 0.9 (300 K)	—	—	[107]
PEDOT:PSS	SWCNT (DMSO)	Film casting	~4000 (95 wt.%)	14–26	~140 (85 wt.%)	0.4–0.7	0.03 (40 wt.%) (300 K)	[108]
PEDOT:PSS	Tos	Film casting	6×10^{-4}–300	40–780	—	0.37	0–0.25 (300 K)	[109]
PEDOT:PSS	Te	Films	19.3 ± 2.3	163 ± 4	70.9	0.22–0.30	0.10 (300 K)	[110]

Table 1.
A summary of the TE properties for eight representative conjugated polymer-based thermoelectrics [101].

Semicrystalline nanocomposites of PEI/SWCNT (10 vol.%) reached a maximum power factor of ~1.8 μW m^{-1} K^{-2}.

In a polymer (insulating or conjugated) matrix, nanoinclusions have the ability to allow electron (n-doping) or hole (p-doping) transport by a plausible tunneling or hopping mechanism, while at the same time, phonon scattering occurs at the nanoparticle-polymer-nanoparticle interfaces preventing their effective transmission and resulting in low thermal conductivities. Therefore, nanocomposites are considered as promising TE materials for thermoelectric power generation (used for the fabrication of TEGs), and a continuous demand remains for the increase of their electrical conductivity, Seebeck coefficient and power factor values compared to existing reported values.

Figure 5a shows the mechanism that governs the TE mechanism of a polymer nanocomposite, and **Figure 5b** depicts a representative transmission electron microscopy (TEM) image of a polymer/CNT TE nanocomposite showing the dispersed 1D nanoparticulates within the polymer matrix (from the author's personal microscopy investigation result data).

Besides, carbon nanomaterials as thin films and thick self-standing films (buckypapers) have been reported also as thermoelectrics. CNTs, for instance, are well-known for their semiconductor electronic properties and have shown thus promising TE performance. Their TE efficiency has been found to be enhanced by the level of doping [92, 93], as well as the dopant nature [34, 36, 39, 90, 94–97]. Doping of the SWCNTs by using, e.g. polyethyleneimine or hexafluoroacetone [98, 99], resulted in Seebeck coefficients up to −50 μV/K. Hewitt et al. reported Seebeck coefficients of CNT buckypapers between 11 and 19 μV/K and also discussed the dependence of the Seebeck coefficient on the CNT acidic treatment protocol [92]. Recently, Dörling et al. demonstrated that nitrogen-doping of the CNT graphitic lattice results in n-type TE behaviour [100].

Table 1 summarizes the electrical conductivity, Seebeck coefficient, thermal conductivity, power factor and *ZT* of different representative conjugated polymer-based TE materials with or without nanoinclusions.

4. Working principle and specific architectures of thermoelectric generators

Thermoelectric generators (TEGs) convert heat into electricity through the Seebeck effect. An applied temperature gradient across the generator will force heat to flow from the hot to the cold side by thermal conduction, while some of this heat is converted to electricity. The possibility of converting a heat flux into an electrical current is realized by a TEG device (schematically illustrated in **Figure 6a**), while the opposite phenomenon is realised by a thermoelectric cooler (TEC) or Peltier device (**Figure 6b**). Regarding the Seebeck effect, when the junctions at the top are heated and those at the bottom are cooled, a temperature difference will occur. The electron/hole pairs are created at the hot end by absorbing heat and then recombined and liberated heat at the cold end. Driven by the mobility of hole/electron, the Seebeck voltage generates between the two ends, resulting in a current flow. As for the process of TE cooling or "Peltier effect", when a voltage is applied across a p/n junction, electron/hole pairs are generated in the vicinity of the junction and flow away, leading to the cooling of the junction on one end and the heating on the other end.

For an ideal TE device with constant TE properties, the maximum heat to electrical power conversion efficiency (η_{max}) and the output power density (P_{max}) are expressed as

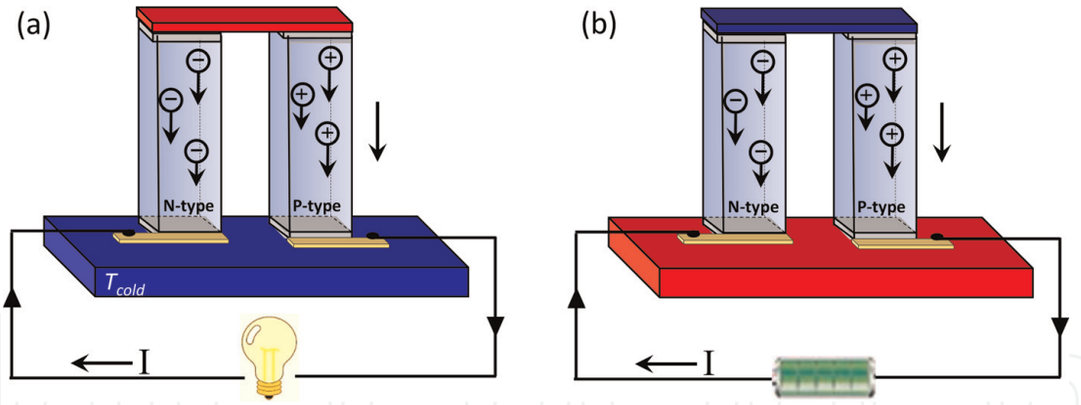

Figure 6.
Operation principle of a (a) thermoelectric generator (TEG) and (b) Peltier device. A TE device generally consisted of p- and n-type TE materials connected in series through conducting plates.

$$n_{max} = \frac{T_H - T_C}{T_H} \bullet \frac{\sqrt{1+\overline{ZT}} - 1}{\sqrt{1+\overline{ZT}} + \frac{T_c}{T_h}} \tag{7}$$

$$P_{max} = \frac{(T_H - T_C)^2}{4L} \bullet \overline{S^2\sigma} \tag{8}$$

where L is the length of the TE leg and T_C and T_H are the cold-side and hot-side temperatures, respectively.

The cooling efficiency of a TE cooling device is characterized by the coefficient of performance (COP):

$$COP = \frac{T_C}{T_{H-T_C}} \frac{\sqrt{1+\overline{ZT}} - \frac{T_H}{T_C}}{\sqrt{1+\overline{ZT}} + 1} \tag{9}$$

The term $\overline{ZT}$ [otherwise reported as ZT_M with T_M the average temperature $T_M = (T_H + TC)/2$] is the average value of ZT, the TE device figure of merit, between the hot and cold sides and is defined by Eq. (10):

$$ZT = \frac{S^2}{RK} \bullet T \tag{10}$$

where S, R, K and T are Seebeck coefficient, electrical resistance, thermal conductance and absolute temperature. Another expression of COP is described by Eq. (11):

$$COP = \frac{S\,T_C I - \frac{I^2R}{2} - K\Delta T}{S\,I\,\Delta T + \frac{I^2R}{2}}, \Delta T_{max} = \frac{Z\,T_H^2}{2} \tag{11}$$

where I is the current, R is the resistance and K is the thermal conductance. If 20°C of cooling is required, the COP would typically be in the region of 2. For comparison, a conventional refrigerator under the same circumstances has a COP of around 14. The maximum temperature difference possible for a TE cooler, ΔT_{max}, is often around 50 K.

If the module is used as a heat pump, the COP_{max} of TE heat pump is given by Eq. (12):

$$COP = S\,I\,\Delta T + S\,T_C\,I + \frac{I^2R}{2} - K\Delta T \tag{12}$$

As an example, for a temperature difference of 20°C, the *COP* for a TE heat pump would typically be 3, which is comparable to the *COP* of conventional heat pumps.

Besides, the Peltier effect can be used to create a refrigerator that is compact and has no circulating fluid or moving parts. Such refrigerators are useful in applications where their advantages outweigh the disadvantage of their very low efficiency. The Peltier effect is also used by many thermal cyclers, laboratory devices used to amplify DNA by the polymerase chain reaction (PCR). Finally, thermocouples and thermopiles are devices that use the Seebeck effect to measure the temperature difference between two objects. Thermocouples are often used to measure high temperatures, holding the temperature of one junction constant or measuring it independently (cold junction compensation). Thermopiles use many thermocouples electrically connected in series, for sensitive measurements of very small temperature difference.

5. Application of thermoelectric generators (TEGs) for power generation

A TEG is typically used for energy transduction through the Seebeck effect. TEG devices display a variety of advantages compared to other common energy technologies. TEGs function like heat engines but are less bulky and have no moving parts, no noise and long operating lifetime; however, they are typically more expensive and less efficient.

TEGs have wide applications in military, aerospace, cogeneration, medical thermostat, microsensors, etc. They have been used in power plants for converting waste heat into additional electrical power (a form of energy recycling) and in automobiles as automotive thermoelectric generators (ATGs) for increasing fuel efficiency. Space probes often use radioisotope thermoelectric generators (R-TEGs) with the same mechanism but using radioisotopes to generate the required heat difference. Recent uses include body heat—powered lighting and a smartwatch powered by body heat. As examples of TEG applications in the transport sector, e.g. in the aircraft environment, temperature differences can be found in various locations (i.e. between the interior and exterior during flights, near turbines), while in automotive in structural components (e.g. bonnet, between the interior and exterior of the cabin, chassis, exhaust system, etc.). Recently, flexible thermoelectric generators (f-TEGs) have been developed for human body application to power wearable electronic devices with the highest power of 2.28 $\mu W/cm^2$ [111].

6. Recent trends and challenges

6.1 Market of TEGs and recent technologies in TE materials and devices

TEGs for energy harvesting to enable (i) self-powered wireless sensors and (ii) wearable devices have received an exponential growth the last decade. Namely, the annual market for sub-watt TEGs shown in **Figure 7** is expected to grow at a compound annual growth rate of more than 110% over the period 2014 to 2020 [*according to market research firm Infinergia LLC; Grenoble, France*]. In other words the market for these low-power TEGs will be on average more than double each

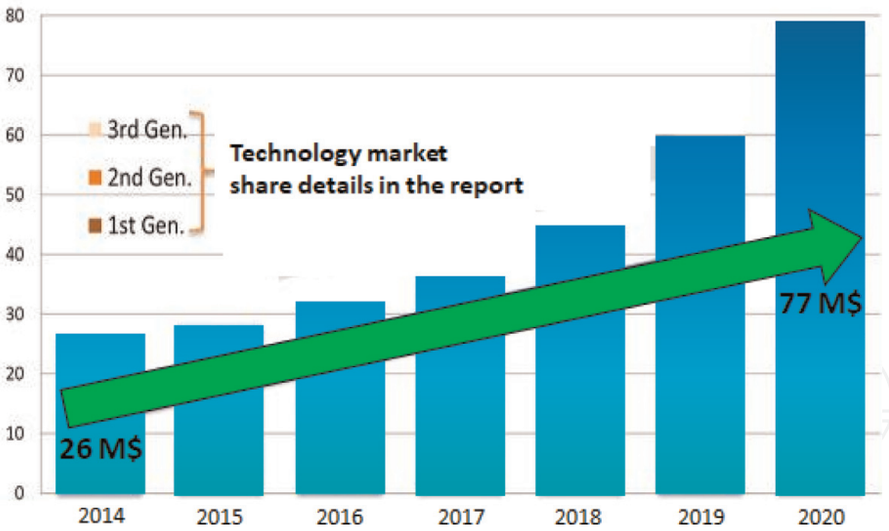

Figure 7.
Annual market size for sub-watt thermoelectric generators (TEGs) with growth at a compound annual growth rate of more than 110% over the period of 2014 to 2020 [according to market research firm Infinergia LLC; Grenoble, France].

year from about 100,000 units shipped in 2014 to about 9 million shipped in 2020. A market size of TEGs considering low-power units is estimated to move from $26 million in 2014 to $77 million in 2020 (thus reaching a CAGR of about 20%).

TEGs are moving into second- and third-generation technologies which are opening up new opportunities, according to Infinergia. Products using sub-watt thermal energy harvesting are being commercialized in several applications across two main segments: (a) infrastructure and buildings and (b) industrial and professional.

The most recent established technology on TE materials and TEGs is related to organic thermoelectrics and organic TEGs (OTEGs). OTEGs can be deposited by vacuum technologies or facile and scalable solution deposition techniques on rigid or flexible substrates (e.g. flexible glass, PET, PEN, etc.). Organic semiconductor materials have advantages of low-cost, lightweight, mechanical flexibility and low-temperature solution processability over large areas, enabling the development of personal, portable and flexible thermal modules. Polymer-based (conducting and nonconducting), nanocarbon-based (CNTs, graphene, fullerenes, etc.) and nanocomposite systems have been reported as TE materials, and in many cases, TEG prototypes have been fabricated to demonstrate their potential for power generation. Critical challenges of organic TE materials include lifetime stability in operation and the relatively low temperatures that can withstand as TE materials. However, the continuous increase of OTEG power output together with a major recent trend of combining TE and photovoltaic devices to maximize the electric energy output [112] comprises a viable avenue for the future market of organic TE materials and OTEGs.

Figure 8 demonstrates a fully printed SWCNT f-TEG (or OTEG) fabricated onto a flexible Kapton polymeric film substrate. Kapton polyimide-based polymer is a high-temperature engineering thermoplastic that exhibits a thermal stability of >500°C [113]. The f-TEG upon being exposed to a temperature gradient of ~110 K creates a thermoelectric voltage output of 41.1 mV. The TEG device demonstrated has been recently fabricated by the sole author of the current book chapter (Dr. Lazaros Tzounis), while more experimental details will be included in scientific publication which is under preparation.

f-TEGs have been reported also based on conventional inorganic low bandgap semiconductor nanomaterials (Bi_2Te_3, PbTe, Ag_2Te_3, etc.) that in the form of

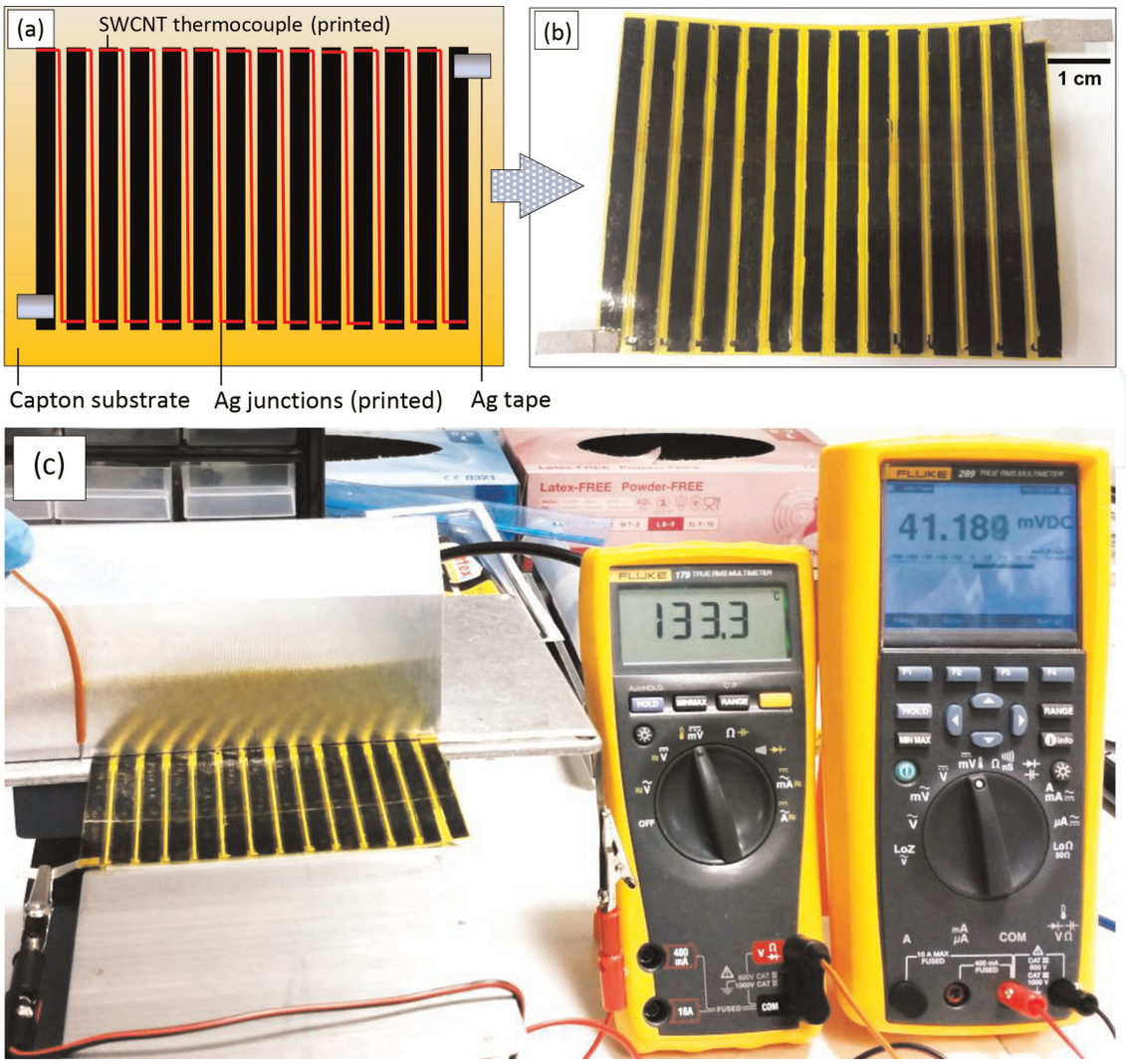

Figure 8.
(a) A carton of a fully printed flexible OTEG with 14 p-type serially interconnected SWCNT thermocouples with Ag junctions, (b) the demonstration of the real device by a digital photo and (c) the f-TEG in operation yielding 41.1 mV upon being exposed to a $\Delta T = \sim 110$ K.

colloidal nanocrystal inks (or pastes) can be printed on various flexible substrates enabling highly efficient TEGs. Printing techniques that have been utilized range from slot-die printing [114], inkjet printing, screen printing [115] to aerosol jet printing [116]. Namely, screen printing technique has been deployed by Varghese et al. [117] to fabricate an f-TEG with high figure of merit onto flexible polyimide substrates. First, bismuth telluride-based nanocrystals have been synthesized using a microwave-stimulated wet chemical method and formulated further as inks. N-type-printed films demonstrated a peak *ZT* of 0.43 along with superior flexibility, which is among the highest reported *ZT* values in flexible thermoelectric materials. A flexible TEG-fabricated device using the printed films exhibited a high power density of 4.1mW/cm^2 at 60°C temperature difference. The additive printing can enable a highly scalable and low-cost roll-to-roll (R2R) manufacturing process to transform high-efficiency colloidal nanocrystals into high-performance and flexible TEG devices for various applications.

Figure 9 demonstrates another potential application of printed f-TEGs by their application underneath flexible photovoltaics (e.g. organic and/or perovskite photovoltaics) in order to increase the total overall efficiency of the hybrid PV-TEG resulting devices. In that case, PVs upon operation and due to light absorbance increase dramatically their temperature at the back contact with the temperature

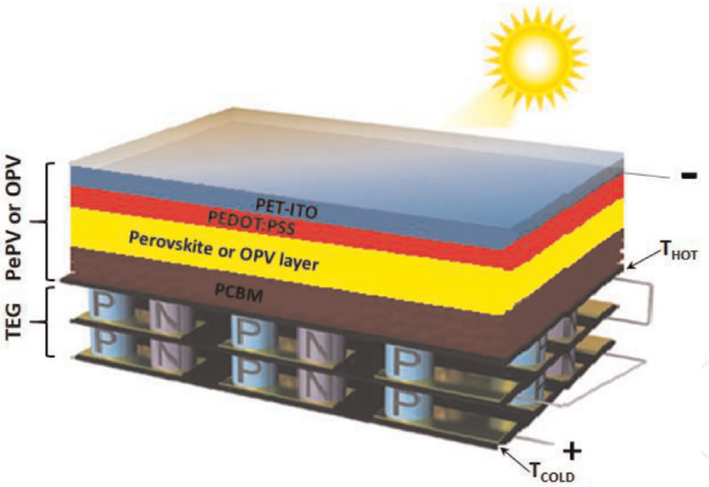

Figure 9.
Demonstration of a hybrid PV-TEG device with an f-TEG coupled with a perovskite or organic photovoltaic towards the increase of the total efficiency.

values rising possibly up to 100–120°C. Therefore, the TEG can utilize this temperature increase as a heat sink and can drive through its other surface-side (cold side) carriers generating Seebeck voltage.

6.2 Challenges in potential TEG application

In order to realize an f-TEG (and any kind of TEG technology) that can power practical devices or for energy harvesting, at least 20 mV should be generated. This value arises from the fact that the voltage output should be generally enhanced via a voltage step-up converter for practical applications (powering of an LED, storage of the harvested energy in a capacitor, etc.). Currently, commercial step-up converters, which are highly integrated DC/DC converters and have no additional power needed, e.g. the LTC3108 (Linear Tech.), operate at inputs of at least 20 mV to give an output voltage of 2.2 V or even higher. Utilizing the LTC3108, Wei et al. [118] powered a light-emitting diode (LED) via a polymer-based f-TEG containing 300 pieces of parallel connected thermocouples (10 in parallel, 30 in series) generating a power output of ~50 μW with an open circuit voltage higher than 40 mV.

Utilizing TEGs with a voltage output of 20–50 mV, with or without a step-up converter driving the DC voltage produced in a capacitor, could enable the powering of low-consumption electronic devices integrated in buildings, e.g. ultra-low-power microcontrollers, wireless sensor networks, etc. [119]. When the TEG produces voltage outputs greater than 100 mV, more sophisticated devices in applications including smart homes and the Internet of things, to name a few, could be powered [120].

7. Future perspectives

There is no doubt that sheet-to-sheet (S2S) printing additive manufacturing technology on planar rigid or flexible substrates will be the most promising technology for TEG fabrication in the future. Printing technology for TEGs is the most rational choice for the fast preparation of thermoelectric films that can be in principle applied, e.g. with ease to hot tubes, whereby one can extract energy from waste heat. The printing techniques can be easily transferred to a high-yield and high-throughput R2R process for scalable and large-scale production of TEGs on flexible substrates.

It is clear that the carrier substrate, which is required for the S2S or R2R processing, leads to a thermal gradient loss as a significant part of the volume is occupied by the carrier. This should be counteracted by employing thinner carrier substrates. A significant improvement should be also considered regarding the maximum possible area usage of the carrier substrate (known also as filling factor—FF).

Related to organic thermoelectric materials and OTEGs, significant improvements by three to four orders of magnitude are required in terms of *ZT*. The sustainable use of organic thermoelectrics from devices with energy payback times comparable with the lifetime of devices is unlikely unless higher thermal gradients can be employed (larger than the temperature range that organic materials can generally endure) [114].

In an attempt to improve the overall energy conversion efficiency, TE devices could be combined with other devices such as solar cells. Many TE materials can be also used in solar cells, such as Si and metal chalcogenides. The wide application of clean solar energy would significantly reduce fossil fuel consumption, our CO_2 footprint, and environmental deterioration, so the use of multiple energy conversion devices to yield maximal output would be an important direction in this area.

It could be envisaged that TEG technology could contribute to (i) the protection of the environment due to the reduction of conventional fuel usage; (ii) strengthen the interfaces between the energy and transport, transmission, and distribution systems; and (iii) promote synergies with the energy/ICT sectors.

8. Summary and conclusions

In this chapter, recent advances in both inorganic and organic TE materials from experimental and theoretical perspectives have been summarized. Detailed *ZT* values for inorganic and organic TE materials were listed in **Table 1**. In most cases, the enhancement of TE performance is attributed to the introduction of nanostructures into the host matrix, including nanoinclusions, nanocomposites, nanowires, nanograins, point defects, etc. Therefore, the development of TE performance depends on the advances in nanoscience and nanotechnology. Nanostructures can significantly reduce thermal conductivity by enhancing the phonon scattering.

The inorganic TE nanomaterials show high performance; however, the following issues have to be solved: (1) large-scale preparation of size, shape and composition; (2) poor stability of nanostructures, as they can be destroyed during compression at high temperature and/or high pressure into pellets; (3) 1D nanowires and 2D nanosheets are limited for large-scale fabrication of TE devices without destroying their nanostructure; and (4) ordered nanostructures are desired, however, not easily achieved in bulk thermoelectrics. Most inorganic TE materials also have issues of high cost or environmental unfriendliness and cannot be processed in large-scale surfaces for TEG fabrication and large-scale thermal energy harvesting (e.g. geothermal energy harvesting, heat exchangers in industrial pipe systems, aeronautics fuselage, etc.).

A great effort has been given in order to highlight the unique potential of organic materials as thermoelectrics and fabricate accordingly OTEG devices. Relatively, carbon materials such as graphene and carbon nanotubes may be promising candidates for further development of lightweight and low-cost polymer composites for TE applications. The generation of thermoelectricity using organic-based structural, engineering polymeric materials (elastomers, thermoplastics, thermosets) that are

routinely exposed to high temperatures can represent a breakthrough in high-performance multifunctional material development.

Acknowledgements

L.T. gratefully acknowledges the Bodossaki Foundation for financial support.

IntechOpen

IntechOpen

Author details

Lazaros Tzounis
Department of Materials Science and Engineering, University of Ioannina, Ioannina, Greece

*Address all correspondence to: ltzounis@cc.uoi.gr

IntechOpen

© 2019 The Author(s). Licensee IntechOpen. This chapter is distributed under the terms of the Creative Commons Attribution License (http://creativecommons.org/licenses/by/3.0), which permits unrestricted use, distribution, and reproduction in any medium, provided the original work is properly cited. CC BY

References

[1] Charisiou ND et al. Syngas production via the biogas dry reforming reaction over nickel supported on modified with CeO_2 and/or La_2O_3 alumina catalysts. Journal of Natural Gas Science and Engineering. 2016;**31**:164-183

[2] Charisiou ND et al. Effect of active metal supported on SiO_2 for selective hydrogen production from the glycerol steam reforming reaction. Bioresources. 2016;**11**:10173-10189

[3] Papageridis KN et al. Comparative study of Ni, Co, Cu supported on γ-alumina catalysts for hydrogen production via the glycerol steam reforming reaction. Fuel Processing Technology. 2016;**152**:156-175

[4] Zhang H et al. A novel phase-change cement composite for thermal energy storage: Fabrication, thermal and mechanical properties. Applied Energy. 2016;**170**:130-139

[5] http://thermoelectrics.matsci.northwestern.edu/thermoelectrics/sustainability.html

[6] Bell LE. Cooling, heating, generating power, and recovering waste heat with thermoelectric systems. Science. 2008; **321**(5895):1457

[7] Volz S. Thermal Nanosystems and Nanomaterials. Berlin Heidelberg: Springer; 2009

[8] Seebeck TJ. Magnetic polarization of metals and minerals. Abhandlungen der Königlichen Akademie der Wissenschaften zu Berlin. 1826;**1823**:265

[9] Peltier JC. Nouvelles expériences sur la caloricité des courants électrique. Annales de Chimie et de Physique. 1834; **56**(14):371-386

[10] Vineis CJ et al. Nanostructured thermoelectrics: Big efficiency gains from small features. Advanced Materials. 2010;**22**(36):3970-3980

[11] Terry MT. Electrical and thermal transport measurement techniques for evaluation of the figure-of-merit of bulk thermoelectric materials. In: Thermoelectrics Handbook. Boca Raton, FL: CRC Press; 2005. pp. 23-1-23-20

[12] Boukai AI et al. Silicon nanowires as efficient thermoelectric materials. Nature. 2008;**451**(7175):168-171

[13] Dresselhaus MS et al. New directions for low-dimensional thermoelectric materials. Advanced Materials. 2007;**19**(8):1043-1053

[14] Pichanusakorn P, Bandaru P. Nanostructured thermoelectrics. Materials Science and Engineering: R: Reports. 2010;**67**(2):19-63

[15] Han C, Li Z, Dou S. Recent progress in thermoelectric materials. Chinese Science Bulletin. 2014;**59**(18): 2073-2091

[16] Snyder GJ, Toberer ES. Complex thermoelectric materials. Nature Materials. 2008;**7**:105

[17] Heremans JP et al. Enhancement of thermoelectric efficiency in PbTe by distortion of the electronic density of states. Science. 2008;**321**(5888):554

[18] Rowe DM. CRC Handbook of Thermoelectrics. Boca Raton, FL: CRC Press; 1995

[19] Hicks LD, Dresselhaus MS. Thermoelectric figure of merit of a one-dimensional conductor. Physical Review B. 1993;**47**(24):16631-16634

[20] Hicks LD, Dresselhaus MS. Effect of quantum-well structures on the thermoelectric figure of merit. Physical Review B. 1993;**47**(19):12727-12731

[21] Tzounis L et al. Controlled growth of Ag nanoparticles decorated onto the surface of SiO_2 spheres: A nanohybrid system with combined SERS and catalytic properties. RSC Advances. 2014;**4**(34):17846-17855

[22] Tzounis L et al. Enhancement of P3HT:PCBM photovoltaic shells efficiency incorporating core-shell Au@Ag plasmonic nanoparticles1. Materials Today: Proceedings. 2016; **3**(3):832-839

[23] Kapnopoulos C et al. Fully gravure printed organic photovoltaic modules: A straightforward process with a high potential for large scale production. Solar Energy Materials and Solar Cells. 2016;**144**:724-731

[24] Kapnopoulos C et al. Gravure printed organic photovoltaic modules onto flexible substrates consisting of a P3HT:PCBM photoactive Blend1. Materials Today: Proceedings. 2016; **3**(3):746-757

[25] Tzounis L et al. Perovskite solar cells from small scale spin coating process towards roll-to-roll printing: Optical and morphological studies. Materials Today: Proceedings. 2017;**4**(4, Part B): 5082-5089

[26] Tzounis L et al. Halloysite nanotubes noncovalently functionalised with SDS anionic surfactant and PS-b-P4VP block copolymer for their effective dispersion in polystyrene as UV-blocking nanocomposite films. Journal of Nanomaterials. 2017;**2017**:11

[27] Gioti M et al. Synthesis, characterization and properties of yellow-light-emitting polyethers containing bis(styryl)anthracene units. AIP Conference Proceedings. 2015; **1646**(1):129-137

[28] Borges BGAL et al. Molecular orientation and ultrafast charge transfer dynamics studies on the P3HT:PCBM blend. The Journal of Physical Chemistry C. 2016;**120**(43):25078-25082

[29] Borges BG et al. Surface, interface and electronic properties of F8:F8BT polymeric thin films used for organic light-emitting diode applications. Polymer International. 2018;**67**:691-699

[30] Wode F et al. Selective localization of multi-wall carbon nanotubes in homopolymer blends and a diblock copolymer. Rheological orientation studies of the final nanocomposites. Polymer. 2012;**53**(20):4438-4447

[31] Tzounis L et al. The interphase microstructure and electrical properties of glass fibers covalently and non-covalently bonded with multiwall carbon nanotubes. Carbon. 2014;**73**: 310-324

[32] Tzounis L et al. High performance natural rubber composites with a hierarchical reinforcement structure of carbon nanotube modified natural fibers. Materials & Design. 2014;**58**:1-11

[33] Liebscher M et al. Influence of the viscosity ratio in PC/SAN blends filled with MWCNTs on the morphological, electrical, and melt rheological properties. Polymer. 2013;**54**(25): 6801-6808

[34] Tzounis L et al. CNT-grafted glass fibers as a smart tool for epoxy cure monitoring, UV-sensing and thermal energy harvesting in model composites. RSC Advances. 2016;**6**(60):55514-55525

[35] Tzounis L et al. Thermal energy harvesting for large-scale applications using MWCNT-grafted glass fibers and polycarbonate-MWCNT nanocomposites. AIP Conference Proceedings. 2015;**1646**(1):138-148

[36] Tzounis L et al. Influence of a cyclic butylene terephthalate oligomer on the processability and thermoelectric properties of polycarbonate/MWCNT

nanocomposites. Polymer. 2014;**55**(21): 5381-5388

[37] Polyzoidis CA et al. Improvement of inverted OPV performance by enhancement of ZnO layer properties as an electron transfer layer. Materials Today: Proceedings. 2016;**3**(3):758-771

[38] Tzounis L et al. All-aromatic SWCNT-polyetherimide nanocomposites for thermal energy harvesting applications. Composites Science and Technology. 2018;**156**: 158-165

[39] Tzounis L et al. Fiber yarns/CNT hierarchical structures as thermoelectric generators. Materials Today: Proceedings. 2017;**4**(7, Part 1): 7070-7075

[40] Tsirka K et al. Production of hierarchical all graphitic structures: A systematic study. Journal of Colloid and Interface Science. 2017;**487**:444-457

[41] Terzopoulou Z et al. Effect of MWCNTs and their modification on crystallization and thermal degradation of poly(butylene naphthalate). Thermochimica Acta. 2017;**656**:59-69

[42] Felisberto M et al. Carbon nanotubes grown on carbon fiber yarns by a low temperature CVD method: A significant enhancement of the interfacial adhesion between carbon fiber/epoxy matrix hierarchical composites. Composites Communications. 2017;**3**:33-37

[43] Carrasco PM et al. Thermoset magnetic materials based on poly(ionic liquid)s block copolymers. Macromolecules. 2013;**46**(5):1860-1867

[44] Tzounis L, Logothetidis S. Fe_3O_4@SiO_2 core shell particles as platforms for the decoration of Ag nanoparticles. Materials Today: Proceedings. 2017;**4**(7, Part 1): 7076-7082

[45] Rowe DM. Recent developments in thermoelectric materials. Applied Energy. 1986;**24**(2):139-162

[46] He J, Liu Y, Funahashi R. Oxide thermoelectrics: The challenges, progress, and outlook. Journal of Materials Research. 2011;**26**(15): 1762-1772

[47] Bubnova O, Crispin X. Towards polymer-based organic thermoelectric generators. Energy & Environmental Science. 2012;**5**(11):9345-9362

[48] Sootsman JR, Chung DY, Kanatzidis MG. New and old concepts in thermoelectric materials. Angewandte Chemie International Edition. 2009; **48**(46):8616-8639

[49] Liu W et al. Recent advances in thermoelectric nanocomposites. Nano Energy. 2012;**1**(1):42-56

[50] Li Z et al. Semiconductor nanowires for thermoelectrics. Journal of Materials Chemistry. 2012;**22**(43):22821-22831

[51] Li Z et al. Formation and function of bismuth nanocatalysts for the solution-liquid-solid synthesis of CdSe nanowires. Small. 2008;**4**(10): 1698-1702

[52] Li J-F et al. High-performance nanostructured thermoelectric materials. NPG Asia Materials. 2010;**2**: 152

[53] Du Y et al. Research progress on polymer–inorganic thermoelectric nanocomposite materials. Progress in Polymer Science. 2012;**37**(6):820-841

[54] Gao C, Chen G. Conducting polymer/carbon particle thermoelectric composites: Emerging green energy materials. Composites Science and Technology. 2016;**124**:52-70

[55] Chen G, Xu W, Zhu D. Recent advances in organic polymer

thermoelectric composites. Journal of Materials Chemistry C. 2017;**5**(18): 4350-4360

[56] He R, Schierning G, Nielsch K. Thermoelectric devices: A review of devices, architectures, and contact optimization. Advanced Materials Technologies. 2017;**3**(4): 1700256

[57] Harman TC et al. Nanostructured thermoelectric materials. Journal of Electronic Materials. 2005;**34**(5): L19-L22

[58] Yan H, Sada N, Toshima N. Thermal transporting properties of electrically conductive polyaniline films as organic thermoelectric materials. Journal of Thermal Analysis and Calorimetry. 2002;**69**(3):881-887

[59] Kim GH et al. Engineered doping of organic semiconductors for enhanced thermoelectric efficiency. Nature Materials. 2013;**12**:719

[60] Hong W et al. Thermally driven large N-type voltage responses from hybrids of carbon nanotubes and poly (3,4-ethylenedioxythiophene) with Tetrakis(dimethylamino)ethylene. Advanced Materials. 2015;**27**(43): 6855-6861

[61] Poudel B et al. High-thermoelectric performance of nanostructured bismuth antimony telluride bulk alloys. Science. 2008;**320**(5876):634-638

[62] Du Y et al. Simultaneous increase in conductivity and Seebeck coefficient in a polyaniline/graphene nanosheets thermoelectric nanocomposite. Synthetic Metals. 2012;**161**(23–24): 2688-2692

[63] Meng C, Liu C, Fan S. A promising approach to enhanced thermoelectric properties using carbon nanotube networks. Advanced Materials. 2010; **22**(4):535-539

[64] Wang L et al. Thermoelectric properties of conducting polyaniline/ graphite composites. Materials Letters. 2011;**65**(7):1086-1088

[65] Tomlinson EP et al. Tuning the thermoelectric properties of a conducting polymer through blending with open-Shell molecular dopants. ACS Applied Materials & Interfaces. 2015; **7**(33):18195-18200

[66] Yi C et al. Enhanced thermoelectric properties of poly(3,4-ethylenedioxythiophene):poly (styrenesulfonate) by binary secondary dopants. ACS Applied Materials & Interfaces. 2015;**7**(17):8984-8989

[67] Mengistie DA et al. Enhanced thermoelectric performance of PEDOT: PSS flexible bulky papers by treatment with secondary dopants. ACS Applied Materials & Interfaces. 2015;**7**(1): 94-100

[68] Moriarty GP et al. Thermoelectric behavior of organic thin film nanocomposites. Journal of Polymer Science Part B: Polymer Physics. 2013; **51**(2):119-123

[69] Bounioux C et al. Thermoelectric composites of poly(3-hexylthiophene) and carbon nanotubes with a large power factor. Energy & Environmental Science. 2013;**6**(3):918-925

[70] Song H et al. Fabrication of a layered nanostructure PEDOT:PSS/ SWCNTs composite and its thermoelectric performance. RSC Advances. 2013;**3**(44):22065-22071

[71] Anthopoulos TD et al. Air-stable ambipolar organic transistors. Applied Physics Letters. 2007;**90**(12):122105

[72] Boris R et al. Power factor enhancement in solution-processed organic n-type thermoelectrics through molecular design. Advanced Materials. 2014;**26**(21):3473-3477

[73] Schlitz RA et al. Solubility-limited extrinsic n-type doping of a high electron mobility polymer for thermoelectric applications. Advanced Materials. 2014;**26**(18):2825-2830

[74] Shi K et al. Toward high performance n-type thermoelectric materials by rational modification of BDPPV backbones. Journal of the American Chemical Society. 2015; **137**(22):6979-6982

[75] Dazhen H et al. Bismuth interfacial doping of organic small molecules for high performance n-type thermoelectric materials. Angewandte Chemie International Edition. 2016;**55**(36): 10672-10675

[76] Zhang B et al. Promising thermoelectric properties of commercial PEDOT:PSS materials and their Bi_2Te_3 powder composites. ACS Applied Materials & Interfaces. 2010;**2**(11): 3170-3178

[77] Yu C et al. Thermoelectric behavior of segregated-network polymer nanocomposites. Nano Letters. 2009; **9**(3):1283-1283

[78] Choi K, Yu C. Highly doped carbon nanotubes with gold nanoparticles and their influence on electrical conductivity and thermopower of nanocomposites. PLoS One. 2012;**7**(9): e44977

[79] Hewitt CA et al. Multilayered carbon nanotube/polymer composite based thermoelectric fabrics. Nano Letters. 2012;**12**(3):1307-1310

[80] Poehler TO, Katz HE. Prospects for polymer-based thermoelectrics: State of the art and theoretical analysis. Energy & Environmental Science. 2012;**5**(8): 8110-8115

[81] Yao Q et al. Enhanced thermoelectric performance of single-walled carbon nanotubes/polyaniline hybrid nanocomposites. ACS Nano. 2010;**4**(4):2445-2451

[82] Wang L et al. Preparation and thermoelectric properties of polythiophene/multiwalled carbon nanotube composites. Synthetic Metals. 2013;**181**:79-85

[83] Liang B et al. Fabrication and thermoelectric properties of graphene/ composite materials. Journal of Nanomaterials. 2013;**2013**:5

[84] Bubnova O et al. Optimization of the thermoelectric figure of merit in the conducting polymer poly(3,4-ethylenedioxythiophene). Nature Materials. 2011;**10**(6):429-433

[85] Dubey N, Leclerc M. Conducting polymers: Efficient thermoelectric materials. Journal of Polymer Science Part B: Polymer Physics. 2011;**49**(7): 467-475

[86] Luo J et al. Polypropylene-based melt mixed composites with single walled carbon nanotubes for thermoelectric applications: Switching from p-type to n-type by the addition of polyethylene glycol. Polymer. 2017;**108**: 513-520

[87] Papageorgiou DG et al. β-Nucleated propylene–ethylene random copolymer filled with multi-walled carbon nanotubes: Mechanical, thermal and rheological properties. Polymer. 2014; **55**(16):3758-3769

[88] Tzounis L et al. Shear alignment of a poly(styrene-butadiene-styrene) triblock copolymer/MWCNT nanocomposite. Polymer. 2017;**131** (Supplement C):1-9

[89] Antar Z et al. Thermoelectric behaviour of melt processed carbon nanotube/graphite/poly (lactic acid) conductive biopolymer nanocomposites (CPC). Materials Letters. 2012;**67**(1): 210-214

[90] Liebscher M et al. Influence of the MWCNT surface functionalization on the thermoelectric properties of melt-mixed polycarbonate composites. Composites Science and Technology. 2014;**101**(0):133-138

[91] Liebscher M et al. Thermoelectric energy harvesting with highly conductive CNT-filled polycarbonate composites prepared by melt-mixing. In: 6th International Conference on Carbon Nanoparticle based Composites; Dresden. 2013

[92] Hewitt CA, Carroll DL. The effects of acid treatment on the thermoelectric power of multiwalled carbon nanotubes synthesized by chemical vapor deposition. Chemical Physics Letters. 2013;**580**(Supplement C:67-72

[93] Zhao W et al. Flexible carbon nanotube papers with improved thermoelectric properties. Energy & Environmental Science. 2012;**5**(1): 5364-5369

[94] Tan XJ et al. Thermoelectric properties of ultrasmall single-wall carbon nanotubes. The Journal of Physical Chemistry C. 2011;**115**(44): 21996-22001

[95] Kong WJ et al. Thermoelectric power of a single-walled carbon nanotubes strand. Journal of Physics: Condensed Matter. 2005;**17**(12):1923

[96] Kunadian I et al. Thermoelectric power generation using doped MWCNTs. Carbon. 2009;**47**(3):589-601

[97] Nonoguchi Y et al. Systematic conversion of single walled carbon nanotubes into n-type thermoelectric materials by molecular dopants. 2013;**3**: 3344. DOI: 10.1038/srep0334

[98] Piao M et al. Thermoelectric properties of single walled carbon nanotube networks in polycarbonate matrix. Physica Status Solidi (b). 2013; **250**(8):1468-1473

[99] Piao M et al. Increasing the thermoelectric power generated by composite films using chemically functionalized single-walled carbon nanotubes. Carbon. 2013;**62** (Supplement C):430-437

[100] Dörling B et al. Exploring different doping mechanisms in thermoelectric polymer/carbon nanotube composites. Synthetic Metals. 2017;**225**(Supplement C): 70-75

[101] Xuan Y et al. Thermoelectric properties of conducting polymers: The case of poly(3-hexylthiophene). Physical Review B. 2010;**82**(11):115454

[102] Han S et al. Morphology and thermoelectric properties of graphene nanosheets enwrapped with polypyrrole. RSC Advances. 2014;**4**(55): 29281-29285

[103] Lu Y, Song Y, Wang F. Thermoelectric properties of graphene nanosheets-modified polyaniline hybrid nanocomposites by an in situ chemical polymerization. Materials Chemistry and Physics. 2013;**138**(1):238-244

[104] Toshima N, Imai M, Ichikawa S. Organic-inorganic nanohybrids as novel thermoelectric materials: Hybrids of polyaniline and bismuth(III) telluride nanoparticles. Journal of Electronic Materials. 2011;**40**(5):898-902

[105] Xu K, Chen G, Qiu D. Convenient construction of poly(3,4-ethylenedioxythiophene)-graphene pie-like structure with enhanced thermoelectric performance. Journal of Materials Chemistry A. 2013;**1**(40): 12395-12399

[106] Kim GH, Hwang DH, Woo SI. Thermoelectric properties of nanocomposite thin films prepared with poly(3,4-ethylenedioxythiophene) poly

(styrenesulfonate) and graphene. Physical Chemistry Chemical Physics. 2012;**14**(10):3530-3536

[107] Zhang K, Zhang Y, Wang S. Enhancing thermoelectric properties of organic composites through hierarchical nanostructures. Scientific Reports. 2013; **3**:3448

[108] Moriarty GP, De S, King PJ, Khan U, Via M, King JA, et al. Thermoelectric behavior of organic thin film nanocomposites. Journal of Polymer Science Part B: Polymer Physics. 2013; **51**(2):119-123

[109] Khan ZU et al. Acido-basic control of the thermoelectric properties of poly (3,4-ethylenedioxythiophene)tosylate (PEDOT-Tos) thin films. Journal of Materials Chemistry C. 2015;**3**(40): 10616-10623

[110] See KC et al. Water-processable polymer−nanocrystal hybrids for thermoelectrics. Nano Letters. 2010; **10**(11):4664-4667

[111] Kim CS et al. Structural design of a flexible thermoelectric power generator for wearable applications. Applied Energy. 2018;**214**:131-138

[112] Lee JJ et al. All organic-based solar cell and thermoelectric generator hybrid device system using highly conductive PEDOT:PSS film as organic thermoelectric generator. Solar Energy. 2016;**134**:479-483

[113] McKeen L. 6—Polyimides. In: The Effect of Sterilization on Plastics and Elastomers. 3rd ed. Boston: William Andrew Publishing; 2012. pp. 169-182

[114] Søndergaard Roar R et al. Practical evaluation of organic polymer thermoelectrics by large-area R2R processing on flexible substrates. Energy Science & Engineering. 2013; **1**(2):81-88

[115] Han C et al. High-performance PbTe thermoelectric films by scalable and low-cost printing. ACS Energy Letters. 2018;**3**(4):818-822

[116] Ou C et al. Fully printed organic–inorganic nanocomposites for flexible thermoelectric applications. ACS Applied Materials & Interfaces. 2018; **10**(23):19580-19587

[117] Varghese T et al. High-performance and flexible thermoelectric films by screen printing solution-processed nanoplate crystals. Scientific Reports. 2016;**6**:33135

[118] Wei Q et al. Polymer thermoelectric modules screen-printed on paper. RSC Advances. 2014;**4**(54): 28802-28806

[119] Shi Y et al. A novel self-powered wireless temperature sensor based on thermoelectric generators. Energy Conversion and Management. 2014;**80**: 110-116

[120] Xin L, Shuang-Hua Y. Thermal energy harvesting for WSNs. In: 2010 IEEE International Conference on Systems, Man and Cybernetics. 2010